

Observation via cathodoluminescence of static and sliding damage in sapphire crystals

YUJI ENOMOTO, KAZUSHI YAMANAKA

Mechanical Engineering Laboratory, Namiki 1-2, Sakura-mura, Niihari-gun, Ibaraki, Japan

Surface damage in sapphire crystals was effected by static and sliding contact and then observed using a scanning electron microscope in both the cathodoluminescence and secondary electron modes. It was found that enhanced luminescence appeared at the area of contact damage, and that the luminescence observed might have been associated with point defects generated during the plastic deformation process. The cathodoluminescence images of sliding damage correlated well with the characteristic frictional properties of sapphire crystals.

1. Introduction

Studies on the plastic deformation and fracture behaviour of brittle solids, produced by both static and sliding contact with a hard solid, provide basic ideas on the characteristic friction/wear phenomena and grinding process of these materials. Single crystals such as MgO represent the most attractive simplified system for carrying out such studies.

The cathodoluminescence (CL) mode in a scanning electron microscope has sometimes provided a versatile method for such an investigation using MgO crystals, since it is known that a high increase in blue CL emission occurs from plastically deformed zones. Previous studies have concentrated on CL behaviour in the slip band [1], and in the region surrounding both an indentation [2-5] and a scratched area [6]. In these studies, special attention has been paid to the exact mechanisms causing CL in deformed MgO crystals [2-4, 7, 8]. Although some uncertainty about the cause has remained, particular features of deformation and microfracture, which would not have been made clear without using this technique, have been well illustrated in relation to the frictional behaviour of both single-crystal and polycrystalline MgO [9].

Though a similar enhancement of CL intensity in a deformed zone, as in the case of MgO crystals, has been observed in sapphire crystals [9], little study has been made of the CL behaviour after contact damage in sapphire crystals. The present paper further examines the CL behaviour of pure sapphire in a plastically deformed zone under static and sliding contact.

2. Experimental details

Pure synthetic sapphire (α -alumina crystal) plates were obtained from Toshiba Denko Ltd, with their (0001) basal plane having a mirror-polished surface. First, Knoop indentations were made on their basal plane. Here, scratch tests, using diamond hemispheres with 50 and 100 μm tip radii, were conducted in air at a sliding speed of 0.6 mm sec^{-1} under various loads ranging from 2 to 17.6 N. After each test, the rear side of the scratched face of the specimen was gapped using a diamond wire-saw cutter normal to the scratched track to beneath a certain depth, and then fractured.

Also, repeated slidings on the basal plane in the $[10\bar{1}0]$ direction, and on the prismatic plane in the $[0001]$ direction, of sapphire against a sapphire ball of 3 mm in diameter were made in air under a load of 9.8 N, at a sliding speed of 2 mm sec^{-1} and with a repeated traversal of 2000 cycles. Each time, the specimen was sputter-coated with a thin gold film. The sliding damage was then observed using the CL and secondary electron (SE) modes of a scanning electron microscope (JEOL; JSM-35C). The details of the CL detection apparatus have been reported at length elsewhere [10]. The CL observation and analysis here was conducted at room temperature, with an accelerating voltage of 25 kV and in electron beam absorption current of about 10^{-9} A.

3. Results and discussion

Figs. 1 and 2 show the SE and CL images of contact damage on the (0001) basal face of a sapphire crystals, caused by static loading with a Knoop

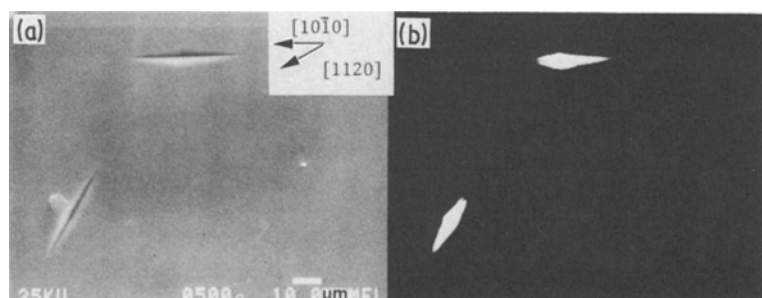


Figure 1 (a) SE and (b) CL images of damage on the (0001) basal face of sapphire crystal, produced by Knoop indentation under a load of 4.9 N.

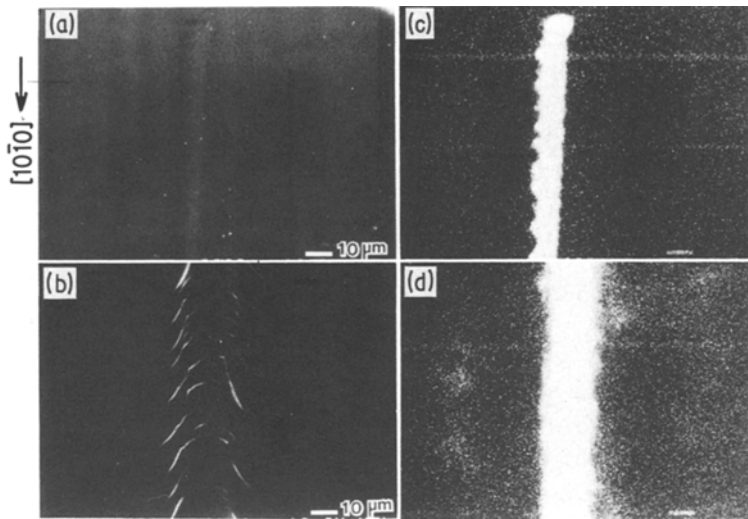


Figure 2 (a, b) SE and (c, d) CL images of damage on the basal face in the $[10\bar{1}0]$ direction of a sapphire crystal, produced by a diamond sphere of $50\ \mu\text{m}$ radius under loads of 1.6 and 3.1 N, respectively.

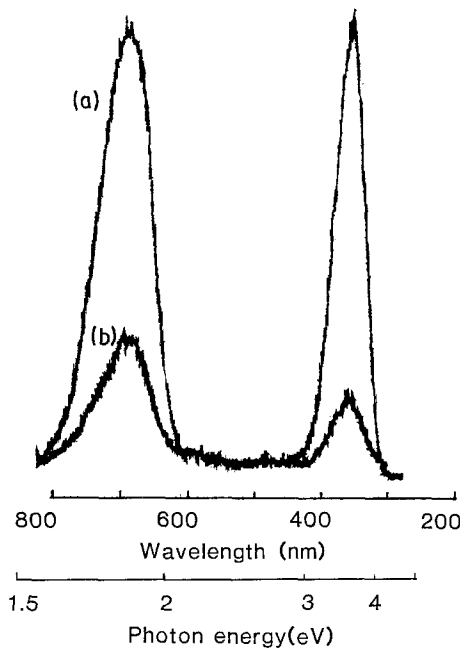


Figure 3 CL spectrum from (a) the centre and (b) the outside of the indentation.

indenter and by sliding with a diamond hemisphere of $50\ \mu\text{m}$ tip radius, respectively. Enhanced luminescence appearance in these contact zones, produced by both static and sliding loading. The extent of fracture associated with the indentation and scratching under a load of 1.5 N is negligible. The main CL of sapphire crystals is, therefore, associated with plastic deformation, as with MgO crystals. As shown in Fig. 3, the spectrum of the sapphire CL emission showed two bands at 332 nm (3.8 eV) and 662 nm (1.9 eV). The intensity of both bands increased substantially with increasing electron irradiation, which indicates an increase in the number of luminescent centres.

It has been observed that the 3.8 eV emission of sapphire crystals is stimulated with light having energy corresponding to absorption bands (6.1, 5.4, 4.8 and 4.1 eV) created by corpuscular-type irradiation (electrons, neutrons and ions) [11–13]. The absorption bands and 3.8 eV emission have been attributed to either F-centres (oxygen-ion vacancies occupied by two electrons) [11] or interstitial aluminium ions [12, 13]. Springis and Valbis [13] recently proposed an energy level diagram for the Al_i^+ centre to explain the observed luminescence absorption and emission

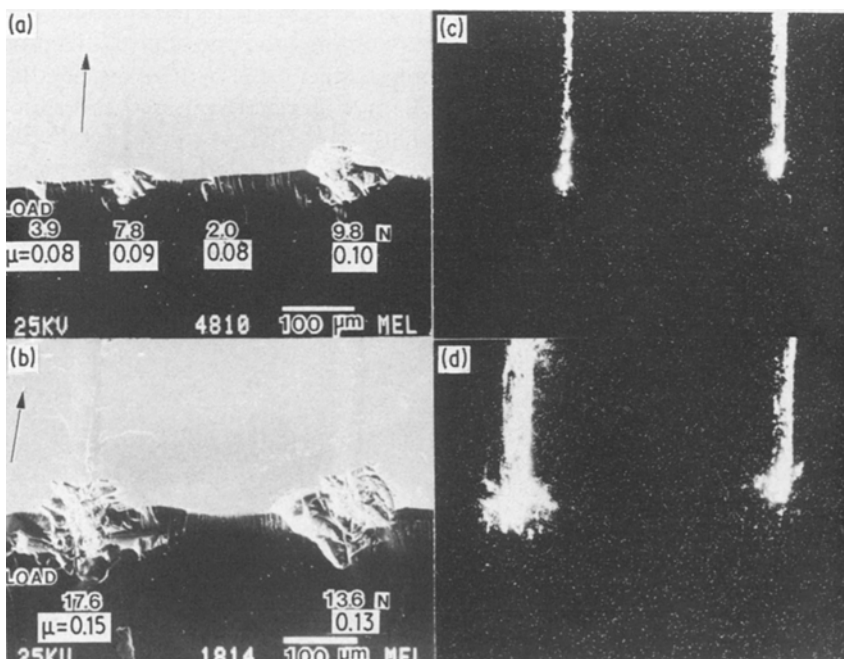


Figure 4 (a, b) SE and (c, d) CL images of damage on the basal face of a sapphire crystal, produced by a diamond hemisphere of $100\ \mu\text{m}$ radius under various loads ranging from 2.0 to 17.6 N.

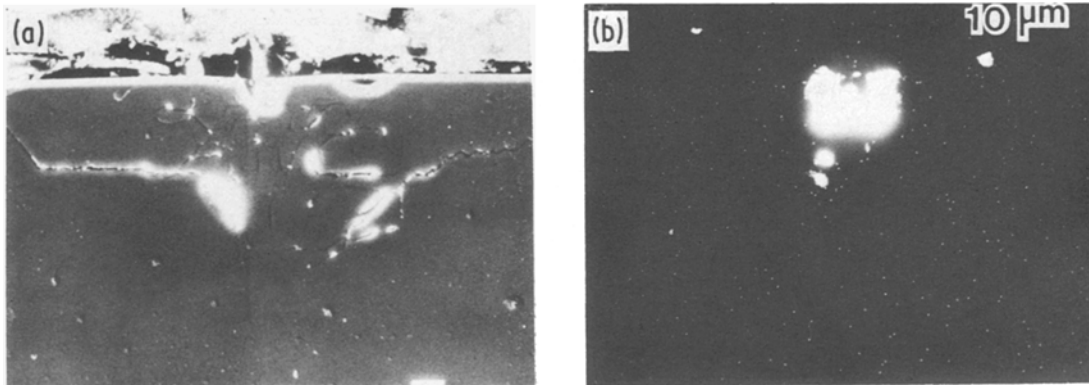


Figure 5 (a) SE and (b) CL images of the cross-sectional view of subsurface damage beneath the track under a load of 13.9 N.

bands. Since the 3.8 eV peak for photoluminescence is equal to that for the cathodoluminescence observed, it is likely that both luminescences are due to electronic transitions within the same defects. The CL band observed at 1.9 eV has not been reported.

Though there is still some controversy about the exact mechanism causing luminescence, it is most probably that these defects are produced during deformation, since the enhancement of luminescence is localized around the plastically deformed zone at the indentation (see Fig. 1)

Steijn [14] found that sapphire crystals undergo plastic deformation via the operation of basal and prismatic slip systems in room-temperature sliding tests, although in conventional deformation tests these slip systems do not operate until a very high temperature of more than 1000°C is reached. During plastic deformation, therefore, intersections of dis-

locations (screw components) are likely to occur and generate point defects, which might be responsible for the luminescence observed around the indentations and track as seen in Figs. 1 and 2.

The relationship between sliding damage and frictional characteristics was investigated next. Fig. 4 shows the SE and CL images of sliding damage on a sapphire crystal's (0001) based face, produced by a diamond rider with a tip radius of 100 μm, under various loads ranging from 2.0 to 17.6 N. The measured values of the coefficient of friction are shown in Figs. 4a and b. It should be noted that below certain critical loads of 2 and 3.9 N the track is essentially non-luminescent. In this load range, the coefficient of friction is independent of applied load, at about 0.8. The track cannot be seen under a conventional optical microscope, thus indicating that the contact is essentially elastic. On the other hand, enhanced luminescence appears in the track above the critical load. In this load range, the coefficient of friction increases with the value of 0.8 with increasing load. The strain a/R (where a is the track half-width and R the tip radius) was in the range 0.15 to 0.3. The scratch hardness ($2P/\pi a^2$) was about 20 GPa. The specimen in Fig. 4 was polished to reveal subsurface damage in a cross-section normal to the track. An example of the cross-sectional view of subsurface damage is shown in Fig. 5. There is a well-defined, plastically deformed luminous zone beneath the track of the rider. It can be seen that the subsurface fracture zone extends deeper than the luminous zone, and that the lateral crack trace is very clearly observed. Over the experimental range investigated, as shown in Fig. 6, the depth of the luminous zone increases linearly with increasing load above a certain critical load. Further study of the energy balance between the frictional work and plastic work done in the luminous zone will be reported in a separate paper.

Finally, the effect of orientation on sliding damage was examined. Fig. 7 shows the SE and CL images of sliding damage on the basal plane along the $[10\bar{1}0]$ direction, and the prismatic plane in the $[0001]$ direction, rubbed against a sapphire ball of 3 mm diameter with a repeated traversal of 2000 cycles under a load of 9.8 N in air. The sliding conditions were the same in both cases. It is known that sapphire wear resistance depends on crystallographic orien-

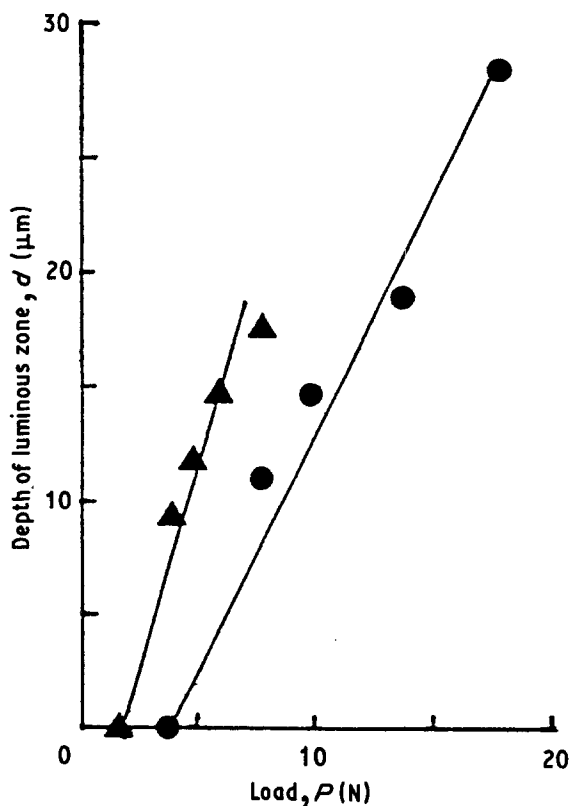


Figure 6 Depth of the luminous zone beneath the track as a function of load. Tip radius: (▲) 50 μm, (●) 100 μm.

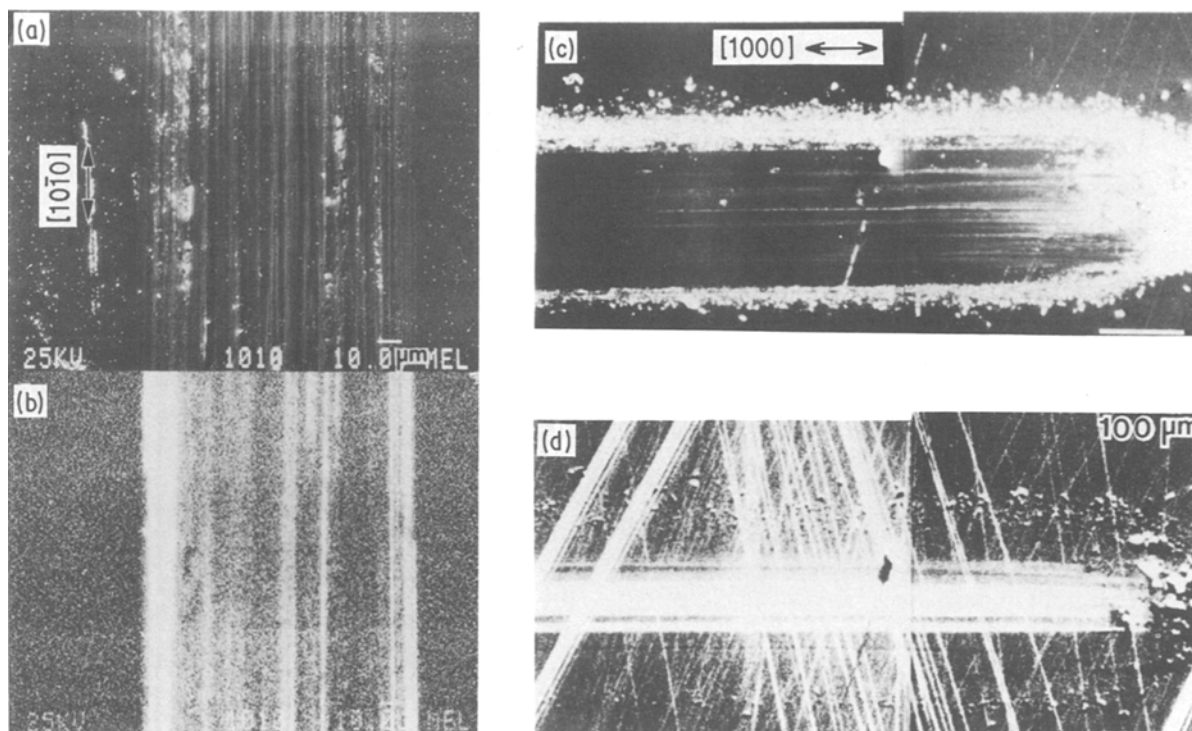


Figure 7 (a, c) SE and (b, d) CL images of damage on the basal plane in (a, b) the $[10\bar{1}0]$ direction and (c, d) the prismatic plane in the $[1000]$ direction of sapphire, produced by a sapphire ball of 3 mm diameter after a repeated traversal of 2000 cycles under a load of 9.8 N, in air.

tation; the basal plane is the weakest crystal face [14]. This aspect is clear when the CL image of sliding damage on the basal plane is compared with that of the damage on the prismatic plane in Figs. 7b and d; the luminous zone (i.e. the plastically deformed zone) extends over the sliding track on the basal plane, whereas this zone is localized around the centre of the track on the prismatic plane where the contact pressure is maximum. The coefficient of friction was 0.4 on the basal plane, whereas it was 0.21 on the prismatic plane. It was noted that the prismatic surface showed many luminescent scratch marks which were introduced during the grinding process. The observation of CL images thus provides us with a versatile method for examining any surface damage on luminescent materials caused during a grinding process.

References

1. J. LLOPIS, J. DIQUERAS and L. J. BRU, *J. Mater. Sci.* **13** (1978) 1361.
2. M. A. VELEDNITSKAYA, V. N. ROZHANSKII, L. F. COMOLOVAN, G. V. SAPARIN, J. SCHREIBER and O. BRÜMMER, *Phys. Status Solidi (a)* **32** (1975) 123.
3. S. J. PENNYCOOK and L. M. BROWN, *J. Luminesc.* **18/19** (1978) 905.
4. M. M. CHAUDHRI, J. T. HAGAN and J. K. WELLS, *J. Mater. Sci.* **15** (1980) 1189.
5. Y. ENOMOTO, *Wear* **89** (1983) 19.
6. Y. CHEN, M. M. ABRAHAM, T. J. TURNER and C. M. NELSON, *Phil. Mag.* **32** (1975) 99.
7. S. DATTA, I. M. BOSWARVA and D. B. HOLT, *J. Phys. Chem. Solids* **5** (1979) 567.
8. R. GONZALEZ, J. PIQUERAS and J. LLOPIS, *J. Appl. Phys.* **53** (1982) 7534.
9. Y. ENOMOTO and K. YAMANAKA, in Proceedings of International Conference on Wear of Materials, Reston, Virginia (ASME, 1983) p. 174.
10. Y. ENOMOTO, K. YAMANAKA and K. SAITO, in Proceedings of International Conference on Tribology, Tokyo, 1985 (JSLE, 1985) p. 109.
11. K. H. LEE and J. H. CROWFORD, Jr, *Appl. Phys. Lett.* **33** (1978) 273.
12. E. W. J. MITCHELL, J. D. RIGDEN and P. W. TOWNSEND, *Phil. Mag.* **5** (1960) 1013.
13. M. J. SPRINGIS and J. A. VALBIS, *Phys. Status Solidi (b)* **123** (1984) 335.
14. R. P. STEIJN, *J. Appl. Phys.* **32** (1961) 1951.

Received 13 May
and accepted 12 June 1985